JOURNAL OF VIROLOGY, Mar. 2011, p. 2247–2253 Vol. 85, No. 5
0022-538X/11/$12.00 doi:10.1128/JVI.01796-10

Peroxiredoxin 1 Is Required for Efficient Transcription and Replication of Measles Virus[▽]

Akira Watanabe,[2] Misako Yoneda,[1] Fusako Ikeda,[1] Akihiro Sugai,[1] Hiroki Sato,[1] and Chieko Kai[1,2]*

Laboratory Animal Research Center, The Institute of Medical Science, The University of Tokyo, 4-6-1 Shirokanedai, Minato-ku, Tokyo 108-8639, Japan,[1] and International Research Center for Infectious Diseases, The Institute of Medical Science, The University of Tokyo, 4-6-1 Shirokanedai, Minato-ku, Tokyo 108-8639, Japan[2]

Received 24 August 2010/Accepted 24 November 2010

Measles is a highly contagious human disease caused by the measles virus (MeV). In this study, by proteomic analysis, we identified peroxiredoxin 1 (Prdx1) as a host factor that binds to the C-terminal region of the nucleoprotein (N; N_{TAIL}) of MeV. Glutathione *S*-transferase (GST) pulldown experiments showed that the Prdx1-binding site overlapped with the MeV phosphoprotein (P)-binding site on N_{TAIL} and that Prdx1 competed for the binding to N_{TAIL} with the P protein, which is a component of RNA-dependent RNA polymerase (RdRp). Furthermore, RNA interference for Prdx1 resulted in a significant reduction in MeV growth in HEK293-SLAM cells. A minigenome assay indicated that Prdx1 suppression affected the viral RNA transcription and/or replication step. Relative quantification of viral RNA by real-time PCR (RT-PCR) showed that Prdx1 suppression not only reduced viral RNA transcription and replication but also enhanced polar attenuation in viral mRNA transcription. Surface plasmon resonance analysis showed that the binding affinity of Prdx1 to MeV-N was 40-fold lower than that of MeV-P to MeV-N, which suggested that Prdx1 might be involved in the early stage of MeV infection, when the expression level of Prdx1 was much higher than that of MeV-P. Since Prdx1 was expressed abundantly and constitutively in various cells, the results in this study indicate that Prdx1 is one of the inherent host factors implicated in MeV RNA synthesis.

Measles is a highly contagious and very serious human disease caused by the measles virus (MeV). MeV infection causes immunosuppression, which induces secondary infection and several complications, such as diarrhea, pneumonia, and encephalitis. Presently, measles can be prevented by administering live vaccines that are derived mainly from the MeV Edmonston strain (MeV-Ed); however, measles has still been the leading cause of death in children, particularly in developing countries, for the past 40 years (6).

MeV is an enveloped virus with a negative single-stranded RNA genome and belongs to the genus *Morbillivirus* in the family *Paramyxoviridae*. MeV is composed of six structural proteins: nucleoprotein (N), phosphoprotein (P), matrix protein (M), fusion protein (F), hemagglutinin protein (H), and large protein (L). Among these structural proteins, the N, P, and L proteins are essential for viral RNA transcription and replication. The L protein exhibits RNA dependent-RNA polymerase (RdRp) activity and forms a complex with the P protein, which acts as a cofactor of RdRp. The N protein consists of two portions: the N-terminal portion, which is termed the core region, is a highly conserved region and is involved in the oligomerization and encapsidation of genomic RNA, and the C-terminal portion, which is termed the tail region, is a relatively variable and disordered region that binds to the P protein. In paramyxoviruses, the N-genomic RNA complex serves as a template for viral RNA transcription and replication by RdRp composed of P and L proteins. During viral RNA synthesis, the P protein binds to the C-terminal region of the N protein (N_{TAIL}) so that RdRp can be tethered to the ribonucleocapsid and can move on the genomic RNA by transferring to the adjacent N protein, in turn (3, 4). RdRp transcribes viral genes sequentially from the 3′ leader side to the 5′ trailer side of the genomic RNA, and there is attenuation of transcription at each intergenic region, resulting in a gradient of transcripts; this is generally termed polar attenuation (12).

Some host factors have been reported to associate with N protein and to be involved in viral RNA transcription and replication in mononegaviruses. Cyclophilin A (CypA), a chaperon protein possessing peptidyl prolyl *cis-trans* isomerase activity, binds to the N protein of the vesicular stomatitis virus (VSV) and is required for efficient viral replication (1). Hsp72 (20, 29), an inducible heat shock protein, binds to N_{TAIL} of MeV-Ed and competes with the P protein in binding to it (35). The overexpression of hsp72 enhances both viral transcription and genome replication of MeV-Ed in mouse neuroblastoma cells (30, 31) and enhances the viral manipulation and pathogenicity of MeV-Ed in a transgenic mouse model of measles encephalitis (7). It has been proposed that hsp72 loosened the binding of RdRp to the ribonucleocapsid so that RdRp could transfer smoothly to adjacent N_{TAIL}, which allowed viral RNA synthesis to proceed efficiently (35). Hsp72 binds to two regions on N_{TAIL} of MeV-Ed, namely, Box-2 and Box-3. Substitution of Asn 522 on Box-3 found in vaccine strains to Asp found in wild-type strains caused the loss of the interaction between Box-3 and hsp72 and attenuates transcriptional response to hsp72, although the substitution has no effect on the responsiveness of genome replication to hsp72. Furthermore, a non-hsp72-interactive Box-3 sequence (522D) attenuates a significant stimulatory effect of hsp72 on viral progeny release (34).

* Corresponding author. Mailing address: Laboratory Animal Research Center, The Institute of Medical Sciences, The University of Tokyo, 4-6-1 Shirokanedai, Minato-ku, Tokyo 108-8639, Japan. Phone: 81-3-5449-5497. Fax: 81-3-5449-5379. E-mail: ckai@ims.u-tokyo.ac.jp.

▽ Published ahead of print on 15 December 2010.

In this report, we identified peroxiredoxin 1 (Prdx1) (23, 28) as another host factor that binds to MeV N_{TAIL} and is involved in viral RNA synthesis and viral propagation.

MATERIALS AND METHODS

Cell culture, virus, and antibodies. HEK293-SLAM cells, which stably express a marmoset signaling lymphocyte activating molecule (SLAM), were cultured in Dulbecco's modified Eagle medium (DMEM) (Sigma-Aldrich) with 5% fetal bovine serum (FBS). B95a cells were cultured in RPMI with 5% FBS. A recombinant MeV, MeV-luc (32), which is derived from wild-type strain MV-HL (17), was propagated in B95a cells at 37°C in RPMI with 2% FBS. The anti-human peroxiredoxin 1 rabbit polyclonal antibody (Hycult Biotechnologies) was purchased.

Proteomic analysis of MeV-N protein binding protein. COBL-a cells were lysed with a lysis buffer (10 mM HEPES [pH 7.4], 0.15 M NaCl, 0.5% NP-40, protease inhibitor cocktails [BD Biosciences]). The lysate was incubated with 20 μg of His-tagged N_{TAIL} (32) in 300 μl of binding buffer (10 mM HEPES [pH 7.4], 150 mM NaCl, 0.1% NP-40, protease inhibitor cocktails) at 4°C overnight. Two milligrams of chemical cross-linker 3,3′-dithiobis(sulfosuccinimidyl-propionate) (DTSSP) (Pierce) was added to the mixture and reacted on ice for 2 h. Unreacted cross-linkers were inactivated by adding 30 μl of 1 M Tris-HCl (pH 8.0), and then NaCl and imidazole were added to the mixtures, whose final concentrations were 0.5 M and 25 mM, respectively. A total of 40 μl of Ni Sepharose 6 fast flow beads (GE Healthcare) were added to the mixture to trap the complex of N_{TAIL} and cellular proteins. The beads were washed extensively with washing buffer 1 (10 mM HEPES [pH 7.4], 0.5 M NaCl, 25 mM imidazole, 1% Triton X-100) and then with washing buffer 2 (10 mM HEPES [pH 7.4], 0.5 M NaCl, 25 mM imidazole), following incubation with 100 μl of washing buffer 2 containing 200 mM dithiothreitol (DTT) at 4°C overnight. The supernatant in which cellular proteins were released was precipitated with trifluoroacetic acid. The resultant pellet was trypsinized and applied to high-performance liquid chromatography (HPLC)-linked matrix-assisted laser desorption ionization–time of flight mass spectrometry (MALDI-TOF MS). Detected peptides were analyzed by the Mascot search engine.

Purification of recombinant proteins and GST pulldown. For the expression of His-tagged recombinant proteins, the pETE vector was constructed by inserting a linker fragment (sense strand, 5′-CGGTCGAATTCGGATCCGAGCT-3′, and reverse strand, 5′-CGGATCCGAATTCGACCGGTAC-3′) into the KpnI/HindIII site of the pET45b(+) vector (Novagen). The cDNA of human peroxiredoxin 1 (Prdx1) was obtained from the total RNA of HEK293 cells by reverse transcription (RT) with Superscript II reverse transcriptase (Invitrogen) and was followed by a PCR with TaKaRa LA *Taq* polymerase using a specific primer pair corresponding to Prdx1 cDNA (5′-TTGAATTCGGATGTCTTCAGGAAATG CTAAAATTGGGC-3′ and 5′-TTCTCGAGTCACTTCTGCTTGGAGAAAT ATTCTTTGC-3′; restriction sites are underlined). The MeV-P gene was amplified using a specific primer pair (5′-TTGAATTCGGATGGCAGAAGAGCAG GCACGC-3′ and 5′-TTCTCGAGTCAGTCTAGAAGATCTCTGTCATTGTA TAC-3′; restriction sites are underlined). The fragment of N_{TAIL} was amplified using a specific primer pair (5′-TTGAATTCGGACTACTGAGGACAGGATC AGTAG-3′ and 5′-TTCTCGAGTCAGTCTAGAAGATCTCTGTCATTGTAT AC-3′; restriction sites are underlined.). The amplified genes were inserted into the EcoRI/XhoI site of the pETE vector. For the expression of GST-N_{TAIL} and its deletion mutants, each fragment was amplified by PCR using the following primers: 5′-TTGAATTCGGACTACTGAGGACAGGATCAGTAG-3′, 5′-TT GAATTCCCCACGGTGATCAAAGTGAGAATGAG-3′, 5′-TTCTCGAGTC AGTCTAGAAGATCTCTGTCATTGTATAC-3′, 5′-TTCTCGAGTCAACTG TCCTGCGGATCTTGGC-3′, and 5′-TTCTCGAGTCACCTAGGGGTGTCC GTGTCTG-3′ (restriction sites are underlined). The amplified genes were inserted into the EcoRI/XhoI site of the pGEX-4T2 vector (GE Healthcare). His-Prdx1 and His-MeV-P were expressed in BL21(DE3), and His-N_{TAIL} was expressed in Rosetta Blue pLysS (DE3); these were purified with Ni Sepharose 6 fast flow beads (GE Healthcare). GST-N_{TAIL} and its deletion mutants were expressed in Rosetta Blue pLysS (DE3), and each cell lysate was used for the following GST pulldown experiment.

GST pulldown. A total of 40 μl of glutathione Sepharose beads was incubated with 100 μl of cell lysate of GST-N_{TAIL} or its deletion mutants, washed with 50 mM phosphate-buffered saline (PBS; pH 7.4) containing 0.5% NP-40, and incubated with 2 μg of His-Prdx1 on ice for 30 min. After incubation, each sample was washed five times with the PBS containing 0.5% NP-40 and developed by SDS-PAGE. Pulled-down Prdx1 was detected by Western blotting with the anti-His_6 rabbit polyclonal antibody (Santa Cruz) and horseradish peroxidase (HRP)-conjugated anti-rabbit IgG goat polyclonal antibody (Dako). Bait proteins were detected with the anti-GST rabbit polyclonal antibody (Santa Cruz) and HRP-conjugated anti-rabbit IgG goat polyclonal antibody (Dako).

For a competition assay, 0.7 μM His-MeV-P and 0.7 μM GST- N_{TAIL} were incubated in the presence of 0 to 100 μM His-Prdx1 on ice for 1 h. After incubation, each sample was incubated with 40 μl glutathione Sepharose beads on ice for 10 min and then washed five times with the PBS containing 0.5% NP-40. Pulled-down His-MeV-P was detected by Western blotting with the anti-His_6 rabbit polyclonal antibody (Santa Cruz).

Surface plasmon resonance. Purified His-Prdx1 or His-MeV-P was immobilized on CM5 sensor chips (Biacore) by amine coupling. Approximately 1,000 resonance units (RU) of each protein was immobilized. For an analyte, purified His-N_{TAIL} was diluted with HBS-P buffer (Biacore) and applied on the sensor chips. The interaction of each protein and His-N_{TAIL} was monitored by BIACORE X (Biacore).

RNA interference. All small interfering RNAs (siRNAs) were synthesized by *in vitro* RNA synthesis using the RiboMax large-scale RNA purification system (Promega) and RNase TI. The target sequences of siRNAs (11) used in this study were as follows: siCONT, 5′-AAUUCUCCGAACGUGUCACGU-3′; siPrx1-3, 5′-CAGAUGGUCAGUUUAAAGAUA-3′; and siPrx1-4, 5′-CAGCC GAAUUGUGGTGUCUUA-3′.

HEK293-SLAM cells were transfected with 40 nM siRNA and infected with MeV-luc at a multiplicity of infection (MOI) of 0.1 at 24 h after transfection. At 24 hpi, the cells were lysed, and their luciferase activities were measured using Pikkagene (Toyo Ink).

Minigenome assay. For the minigenome assay, negative-sense genomic RNA, in which a firefly luciferase gene is flanked by leader and trailer sequences of MeV (27), was synthesized *in vitro* using the RiboMax large-scale RNA purification system (Promega).

For normalization, the phosphoglycerate kinase (PGK) promoter was amplified from the plasmid pMSCVneo (BD Biosciences) and inserted into the phRG-B vector (Promega) to construct phRL-PGK, which expresses a *Renilla* luciferase under the control of the murine PGK promoter.

HEK293-SLAM cells were infected with vaccinia virus expressing T7 RNA polymerase, following transfection with genomic RNA and supporting plasmids in which N, P, and L genes were inserted downstream of the T7 promoter. For normalization, phRL-PGK was also cotransfected. Eighteen hours posttransfection, the cells were lysed and firefly and *Renilla* luciferase activities were measured using the dual-luciferase reporter assay system (Promega).

Relative quantification of viral RNA by RT-PCR. HEK293 SLAM cells were transfected with 40 nM siRNA targeting Prdx1 or negative-control siRNA. At 24 h posttransfection, HEK293 SLAM cells were infected with MeV-luc at an MOI of 0.1. At 24 hpi, total RNA was extracted from infected cells and reverse transcribed with PrimeScript reverse transcriptase (TaKaRa). Comparisons of the expression levels of viral mRNAs and genomic RNA were performed by real-time PCR (RT-PCR) using SYBR premix Ex *Taq* (TaKaRa). Relative quantification was performed by the cycle threshold ($\Delta\Delta C_T$) method (19). Briefly, C_T values were normalized to 18S rRNA, as ΔC_T, which was determined by the formula $\Delta C_T = C_T$ (target gene) $- C_T$ (18S rRNA). Fold changes was determined by $2^{-\Delta\Delta CT}$, where $\Delta\Delta C_T = \Delta C_T$ (siPrdx1-3) $- \Delta C_T$ (siCONT). Most of the primer pairs used for real-time PCR in this study were previously reported by another group (24): N, CCAGACAAGCCCAAGTGTC and TGTCTAGGG GTGTGCC; P, GAACTCAATCCCGACCTGAA and GCTGTCCTCTGGAA CTGGTC; M, AACGCAAACCAAGTGT and TGAAGGCCACTGCATT; F, ACATACCTACCTGCGG and AGCTTCTGGCCGATTA; H, ACAACACGG ACAGATGACAAG and ACAAGACCCCGTATGAAGGA; L, GTGTGAAA GCGACGAG and TGTTCCACGAAGATCCT; L-Tr, GAGAAACAGATTAT TATGACGGG and CAAAGCTGGGAATAGAAACT; luciferase, AATCCAT CTTGCTCCAACACC and CGTCTTTCCGTGCTCCAA; and 18S, ACTCAA CACGGGAAACCTC and ACCAGACAAATCGCTCCAC.

Overexpression of Prdx1. A wild-type Prdx1 gene was inserted into the pCMV-HA vector (Clontec). HEK293-SLAM cells were transiently transfected with pCMV-HA-Prdx1 or the pCMV-HA empty vector. After 24 h, the HEK293-SLAM cells were infected with MeV-HL at an MOI of 1.0. At 24 hpi, total RNA was extracted from infected cells and reverse transcribed with random primers. Comparison of the expression level of genomic RNA was performed by quantitative real-time PCR using an L-trailer primer pair. 18S rRNA was used as an internal standard.

RESULTS

Identification of Prdx1 as an N_{TAIL}-binding protein. From a cytoplasmic fraction of COBL-a cells, which are human um-

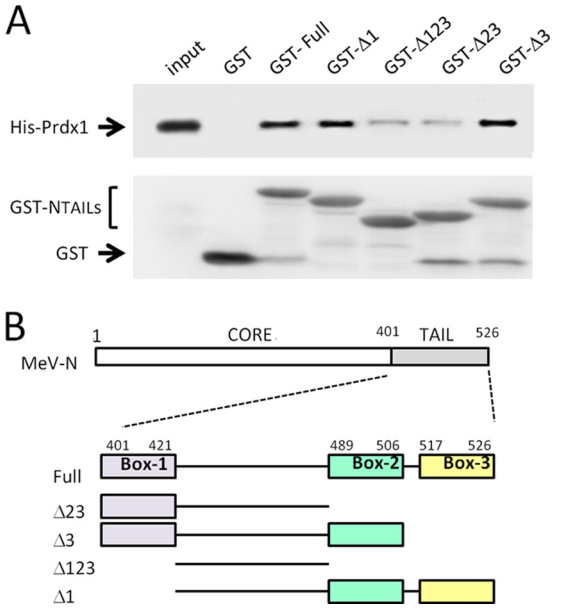

FIG. 1. Identification of the Prdx1-binding region on MeV N_{TAIL}. (A) GST pulldown with His-Prdx1 and GST-N_{TAIL}. GST-N_{TAIL} and its deletion mutants trapped on 40 μl of glutathione Sepharose beads were incubated with purified His-Prdx1 on ice for 30 min. After washing the beads, the sample was subjected to SDS-PAGE, and pulled-down Prdx1 was detected by Western blotting with the anti-His_6 antibody and HRP-conjugated anti-rabbit IgG antibody. Bait proteins were detected with anti-GST antibody and HRP-conjugated anti-rabbit IgG antibody. (B) Construction of deletion mutants of N_{TAIL}. The numbers in the figure indicate the positions of amino acids in full-length MeV-N.

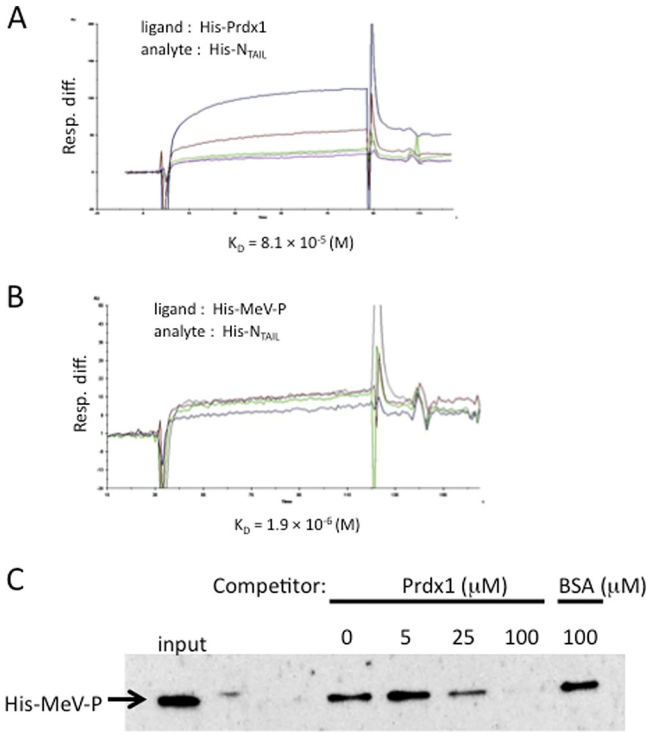

FIG. 2. Comparison of the binding affinity of N_{TAIL} with Prdx1 or the P protein by surface plasmon resonance analysis. Approximately 1,000 RU of purified His-MeV-P or His-Prdx1 was immobilized on CM5 sensor chips as a ligand. Purified His-N_{TAIL} was applied on the sensor chips as an analyte. (A) His-Prdx1 was immobilized as a ligand. Resp. diff., response differential. (B) His-MeV-P was immobilized as a ligand. Colored lines in sensorgrams represent signals from different concentrations of His-N_{TAIL}. (C) Prdx1 competed with the P protein for the binding to N_{TAIL}. Purified GST- N_{TAIL} (0.7 μM) and purified His-MeV-P (0.7 μM) were incubated in the presence of 0, 5, 25, and 100 μM purified His-Prdx1 or 100 μM BSA as a control on ice for 30 min. After incubation, the sample was washed five times with PBS containing 0.5% NP-40 and developed by SDS-PAGE. Pulled-down Prdx1 was detected by Western blotting with the anti-His_6 antibody and HRP-conjugated anti-rabbit IgG antibody. Bait proteins were detected with the anti-GST antibody and HRP-conjugated anti-rabbit IgG antibody.

bilical blood cells susceptible to MeV infection (18), host cellular factors were pulled down using the recombinant N_{TAIL} of MeV-HL (17), which is a wild-type strain, as a bait protein and analyzed by MALDI-TOF MS. By peptide mass fingerprinting, several cellular proteins were identified as N_{TAIL}-binding proteins; one of these was peroxiredoxin 1 (Prdx1) (25), which is a cytosolic antioxidant enzyme.

GST pulldown assay using recombinant Prdx1 and GST-fused N_{TAIL} (GST-N_{TAIL}) revealed that Prdx1 bound to N_{TAIL} directly (Fig. 1A, third lane from left). N_{TAIL} contains three hydrophobic regions, namely, Box-1 (positions 401 to 421), Box-2 (489 to 506), and Box-3 (517 to 526). To address the Prdx1-binding region on N_{TAIL}, deletion mutants of GST-N_{TAIL}, which lacked one or two of the Box regions, were constructed (Fig. 1B). The deletion of Box-1 and/or -3 had little effect on Prdx1-binding ability, while the binding was significantly reduced with deletion of Box-2, although weak binding was still observed (Fig. 1A). These results indicated that Box-2 was a major binding region and that the internal region between Box-1 and Box-2 was a minor binding region for Prdx1.

Prdx1 competes with the P protein for binding to N_{TAIL}. Box-2 of N_{TAIL} is known to bind to the P protein, so that RdRp can be tethered and move on the ribonucleocapsid during viral RNA synthesis (2, 13, 15, 16). Thus, it is possible that Prdx1 prevented the interaction between N_{TAIL} and P.

First, the binding affinities between N_{TAIL} and the P protein or between N_{TAIL} and Prdx1 were estimated by the surface plasmon resonance method. Purified recombinant P protein or Prdx1 was immobilized on a CM5 sensor chip, and purified His tag-fused N_{TAIL} was applied as an analyte. Kinetic analysis showed that the dissociation constant K_D of N_{TAIL}-P binding was 1.9×10^{-6} M, while the K_D of the N_{TAIL}-Prdx1 binding was 8.1×10^{-5} M. This indicates that the binding affinity of Prdx1 for N_{TAIL} was 40-fold lower than that of MeV-P for N_{TAIL} (Fig. 2A, B).

Next, the inhibitory effect of Prdx1 on N_{TAIL}-P binding was examined by a GST pulldown assay. GST- N_{TAIL} (0.7 μM) and MeV-P (0.7 μM) were incubated in the presence of 0, 5, 25, and 100 μM Prdx1. N_{TAIL}-P binding was prevented by Prdx1 in a dose-dependent manner (Fig. 2C); furthermore, 100 μM Prdx1 completely abolished the binding of MeV-P to N_{TAIL}, while 100 μM bovine serum albumin (BSA) showed no inhibitory effects on the binding of the P protein to N_{TAIL}. These results indicate that Prdx1 specifically inhibited N_{TAIL}-P binding, which suggests that Prdx1 might be involved in the regu-

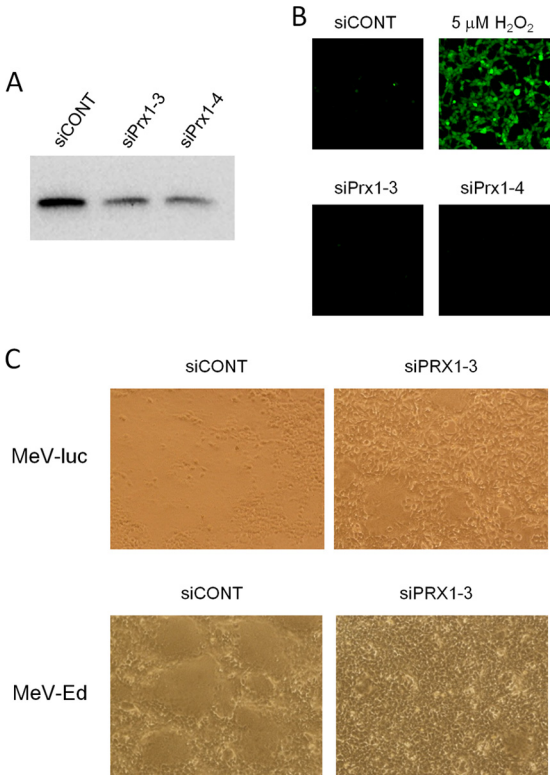

FIG. 3. Prdx1 suppression by RNA interference reduced syncytium formation of MeV. HEK293-SLAM cells were transfected with 40 nM siRNA targeting Prdx1. siPrx1-3 or -4 was an siRNA targeting Prdx1, and siCONT was a negative-control siRNA. (A) At 48 h posttransfection, the cell lysate was subjected to SDS-PAGE followed by Western blotting with the anti-Prdx1 antibody. (B) At 24 h posttransfection, cells were incubated with 5 μM 2′,7′-dichlorofluorescein diacetate (DCF-DA) for 30 min at 37°C. After cells were washed, they were observed by fluorescent microscopy. For a positive control, mock-transfected HEK293-SLAM cells were incubated with 5 μM H_2O_2 at 37°C for 10 min prior to incubation with 5 μM DCF-DA. (C) At 24 h posttransfection of siRNAs, HEK293-SLAM cells were infected with MeV-luc or MeV-Ed at an MOI of 0.1. At 24 hpi, infected cells were observed by microscopy. Size and number of syncytia observed with the cells transfected with siPrx-3 were much smaller than those with the control cells.

lation of viral RNA synthesis by modulating the binding affinity between the nucleocapsid and RdRp.

Prdx1 suppression by RNA interference repressed MeV growth. To analyze the role of Prdx1 on the MeV life cycle, the effect of Prdx1 suppression on MeV growth was examined in HEK293 cells expressing a marmoset SLAM (signaling lymphocyte activating molecule; an MeV receptor) (HEK293-SLAM cells). The expression of Prdx1 was suppressed by transient transfection of siRNAs targeting Prdx1 (siPrx1-3 and -4), and their knockdown efficiencies were at most 50% in HEK293-SLAM cells (Fig. 3A). Since Prdx1 is an antioxidant enzyme that eliminates cellular peroxide (25), the influence of Prdx1 suppression on the oxidative condition of cells was examined by detecting intracellular peroxide using 2′,7′-dichlorofluorescein diacetate (DCF-DA), a peroxide-sensitive dye. As a result, Prdx1 suppression in this study did not cause significant accumulation of intracellular peroxide (Fig. 3B). At 24 h after transfection with siRNAs, HEK293-SLAM cells were infected with MeV-luc, which is an MeV-HL derivative expressing the luciferase gene (32); the luciferase assay was performed at 24 h postinfection (hpi). Prdx1 suppression significantly reduced the number and size of syncytia (Fig. 3C). It has been reported that hsp72 competes with the P protein for the binding to N_{TAIL} of MeV-Ed and that the overexpression of hsp72 enhances viral growth (7, 31, 34). However, the responsiveness to hsp72 is restricted to vaccine strains such as MeV-Ed and does not extend to wild-type strains (34). Thus, the effect of Prdx1 suppression on the viral growth of MeV-Ed, a vaccine strain, was examined. Syncytium formation was significantly inhibited, as in the case of MeV-luc (Fig. 3C). These results indicate that Prdx1 was required for efficient MeV growth in both vaccine and wild-type strains.

Furthermore, the luciferase activity and virus production of MeV-luc-infected cells were significantly reduced by approximately 10-fold (Fig. 4A and B) through Prdx1 suppression.

Minigenome assay. Viral growth is affected by the efficiency of viral entry or the spread by cell fusion, as well as that of viral transcription and replication. Thus, to confirm that the significant reduction of MeV growth by Prdx1 suppression was derived from the viral RNA transcription and replication step, a minigenome assay in which the minigenomic RNA contained a firefly luciferase gene flanked by leader and trailer sequences of MeV was performed (27). At 24 h after the siRNA transfection, HEK293-SLAM cells were infected with a vaccinia virus (VV) expressing a T7 RNA polymerase and then transfected with the minigenomic RNA and supporting plasmids expressing the N, P, and L genes under the control of the T7 promoter. The luciferase assay was performed at 18 h after the transfection of the minigenomic RNA and supporting plasmids. It showed that Prdx1 suppression significantly reduced luciferase activity (Fig. 5), suggesting that Prdx1 was involved in the viral RNA transcription and replication step.

Relative quantification of viral mRNAs and genomic RNA by RT-PCR. To examine the effect of Prdx1 suppression on MeV RNA synthesis, HEK293-SLAM cells were transfected with siPrx1-3 or the control siRNA following MeV-luc infection under the same conditions described above. At 24 hpi, total RNA was extracted, and reverse transcription was performed with a random primer for genomic RNA and with the oligo(dT) primer for mRNAs. A PCR was performed with a primer pair positioned in the open reading frame (ORF) for each viral gene and with an L-trailer primer pair for genomic RNA. The effect of Prdx1 suppression on each viral RNA synthesis was examined by relative quantification using the $\Delta\Delta C_T$ method in qualitative real-time (QRT)-PCR (19). The expression of viral mRNAs and genomic RNA was found to be significantly decreased by Prdx1 suppression, which corresponded to the results of the luciferase assay (Fig. 6). Furthermore, the extent of reduction of viral mRNA expression increased according to the gene order, except for a *luc* mRNA, 51% to 26% (the N to the L gene), suggesting that Prdx1 suppression enhanced the polar attenuation of the transcription. A luciferase gene was inserted between the N and P genes in MeV-luc; however, the extent of reduction of *luc* mRNA expression was much greater than that of P mRNA and similar to that of L mRNA.

Overexpression of Prdx1 also reduced MeV growth. The RNA interference experiment in this study suggested that

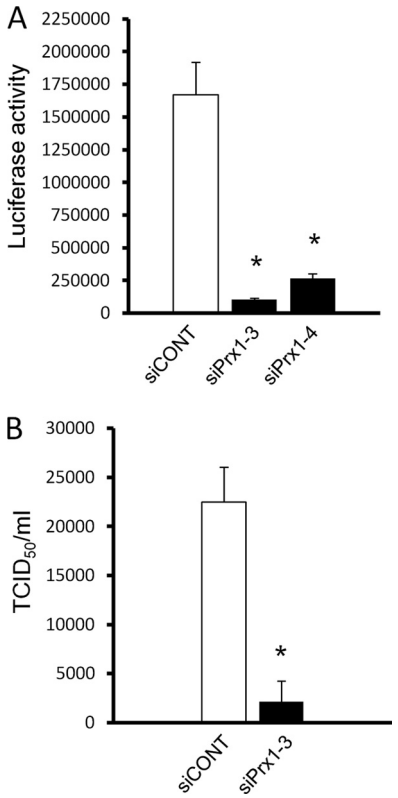

FIG. 4. Prdx1 suppression by RNA interference repressed MeV growth. HEK293-SLAM cells were transfected with 40 nM siRNA targeting Prdx1 or a control siRNA. At 24 h posttransfection, HEK293-SLAM cells were infected with MeV-luc at an MOI of 0.1. (A) At 24 hpi, the luciferase activities of infected cells were examined. The blank and black bars represent the luciferase activity of the control siRNA- and siPrx1-transfected cells, respectively. Luciferase assays were performed in triplicate. The represented data are mean ± standard deviation (SD); *, $P < 0.001$, Student's t test. (B) At 24 hpi, infected cells were sonicated with culture medium. After centrifugation, the viral titer of supernatant was estimated using B95a cells. The blank and black bars represent the viral titer on siCONT- and siPrx1-3-transfected cells, respectively. The represented data are from duplicate experiments and are mean ± SD; *, $P < 0.01$, Student's t test; $TCID_{50}$, 50% tissue culture infective dose.

Prdx1 enhanced MeV growth through its physical interaction with the N protein, independent of its antioxidant activity. To confirm the effect of the physical interaction of Prdx1 with MeV-N on viral growth, HEK293-SLAM cells were transiently transfected with a plasmid expressing Prdx1 and infected with MeV-HL. The effect of Prdx1 overexpression on genomic RNA synthesis was examined by quantitative real-time PCR. Unexpectedly, genomic RNA synthesis showed a tendency to be reduced by the overexpression of Prdx1 ($P = 0.09$) (Fig. 7).

DISCUSSION

Prdx1 is a member of the recently discovered peroxiredoxin family, which comprises thiol-specific antioxidant enzymes that reduce H_2O_2, alkyl hydroperoxides and peroxynitrite using thioredoxin and other peroxiredoxins (22, 26). Furthermore, Prdx1 interacts with the cellular oncogene products c-Abl and c-Myc and inhibits c-Abl kinase activity (33) and c-*myc*-mediated transformation (21) independent of its antioxidant activity; thus, Prdx1 acts as a tumor suppressor.

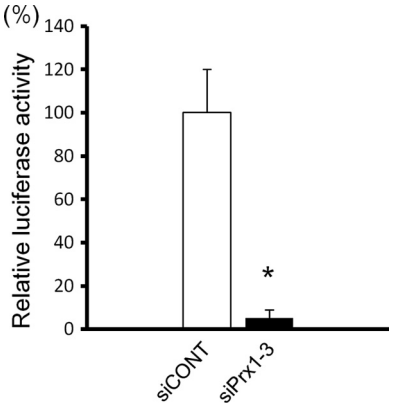

FIG. 5. Effect of Prdx1 suppression on minigenome assay system. At 24 h after transfection with 40 nM siCONT or siPrx1-3, HEK293-SLAM cells were transfected with minigenomic RNA and supporting plasmids. After 18 h, the cells were lysed following the luciferase assay. The blank and black bars represent the relative luciferase activity of the control siRNA- and siPrx1-transfected cells, respectively. Luciferase assays were performed in triplicate. The represented data are the mean ± SD; *, $P < 0.001$, Student's t test.

There have been a few reports on the association between Prdx1 and viruses. It has been reported that Prdx1 was incorporated in the virion of VV, although its role in the VV life cycle is still unknown (9). Prdx1 is also known as natural killer-enhancing factor A (NKEF-A). Previously, it was reported that NKEF-A possessed antiviral activity against human immuno-

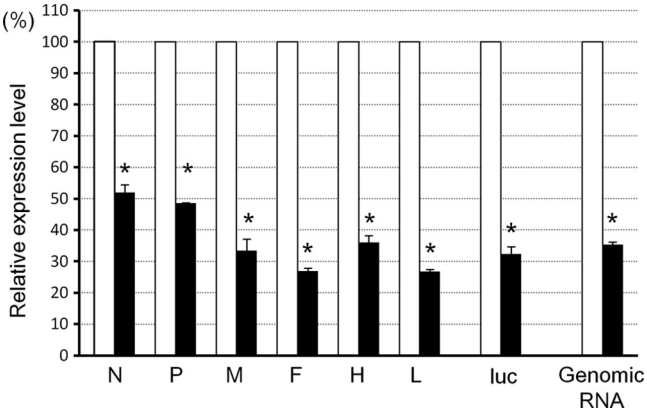

FIG. 6. Effect of Prdx1 suppression on viral RNA synthesis. HEK293-SLAM cells were transfected with 40 nM siCONT or siPrx1-3. At 24 h posttransfection, HEK293-SLAM cells were infected with MeV-luc at an MOI of 0.1. At 24 hpi, total RNA was extracted and reverse transcribed with the oligo(dT) primer for mRNAs or with a random primer for genomic RNA. The relative quantification of each mRNA and the genomic RNA was performed by the $\Delta\Delta C_T$ method in a real-time PCR. For normalization, 18S rRNA was used as an internal standard. The blank and black bars represent the relative expression levels in control siRNA- and siPrx1-3-transfected cells, respectively. The significance was determined between ΔC_T (siCONT) and ΔC_T (siPrdx1-3) in each mRNA for convenience. The represented data are from duplicate experiments and are the mean ± SD; *, $P < 0.00005$, Student's t test.

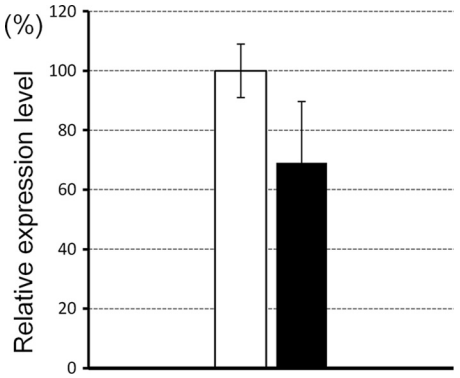

FIG. 7. Effect of overexpression of Prdx1 on MeV growth. At 24 h after transfection with pCMV-HA-Prdx1 or the pCMV-HA empty vector, HEK293-SLAM cells were infected with MeV-luc at an MOI of 1.0. At 24 hpi, total RNA was extracted from infected cells and reverse transcribed with random primers. Comparison of the expression levels of genomic RNA was performed by quantitative real-time PCR using an L-trailer primer pair. For normalization, 18S rRNA was used as an internal standard. The blank and black bars represent relative expression levels of genomic RNA in the cells transfected with the pCMV-HA empty vector and pCMV-HA-Prdx1, respectively. Experiments were performed in duplicate. Represented data are the mean ± SD; $P = 0.09$, Student's t test.

deficiency virus type 1 (HIV-1) by inhibiting HIV-1 transcription through the inactivation of NF-κB (10).

In this study, Prdx1 was identified as a host factor that bound to MeV-N_{TAIL} (Fig. 1). MeV infection did not induce intracellular peroxide in HEK293-SLAM cells at 24 hpi when the N protein was expressed largely in the infected cells (data not shown), which indicated that the binding of N_{TAIL} to Prdx1 had no effect on the oxidative state of infected cells. The GST pulldown experiment revealed that the Prdx1-binding region overlapped with the P protein-binding region on N_{TAIL} and that Prdx1 competed with the P protein for the binding to N_{TAIL} *in vitro* (Fig. 2B). As the binding of the P protein to N_{TAIL} is necessary for the tethering and transfer of RdRp on ribonucleocapsids during viral transcription and replication, these results suggest that physical interaction between N_{TAIL} and Prdx1 may have affected viral RNA synthesis.

To examine the role of Prdx1 in MeV growth, the expression of Prdx1 was suppressed by the transient transfection of siRNAs targeting Prdx1 in HEK293-SLAM cells. Although Prdx1 is an antioxidant enzyme, its suppression did not influence intracellular oxidation or cell viability in HEK293-SLAM cells (Fig. 3B). This is probably because the knockdown efficiency of the siRNAs was at most 50% in this study (Fig. 3). However, the suppression rate of Prdx1 effectively caused a significant reduction in the number and size of syncytia in MeV-luc infection at 24 hpi (Fig. 3C and D), as well as an 80% to 90% reduction in the luciferase activity of infected cells (Fig. 4A). Furthermore, the virus titer was also decreased 10-fold by Prdx1 suppression (Fig. 4B). These results indicate that Prdx1 was positively involved in MeV growth. Although the viral growth was possibly affected by the efficiency of the virus entry and/or cell fusion, as well as by the efficiency of viral RNA transcription and replication, a minigenome assay confirmed that Prdx1 is associated with the viral RNA synthesis step (Fig. 5). QRT-PCR showed that Prdx1 suppression decreased the synthesis of both viral mRNAs and genomic RNA, corresponding to the results of luciferase assay. Furthermore, the extent of reduction of viral mRNA expression increased downstream, 51% to 26% (N to L), which indicated that Prdx1 suppression enhanced the polar attenuation of viral transcription (Fig. 6). It is known that RdRp enters into transcription and replication from the 3′ end of genomic RNA and transcribes viral genes sequentially from the 3′ to the 5′ end. It is believed that RdRp transfers to adjacent N_{TAIL}, in turn, from end to end on ribonucleoprotein, which drives RdRp to advance RNA synthesis, and that the pausing and stopping of the RdRp halfway cause polar attenuation of the transcription (12). Recently, it has been reported that hsp72 bound to MeV-Ed N_{TAIL} and enhanced viral RNA synthesis in mouse cultured cell lines and transgenic mice (8, 31, 35). As hsp72 competes with the P protein for the binding to N_{TAIL}, it is proposed that hsp72 accelerates the transfer of RdRp on ribonucleocapsids by loosening the binding of the P protein to ribonucleocapsids (35). Thus, the results in this study suggested that Prdx1 functions as a driving force for RdRp by modulating the formation of the nucleocapsid-RdRp complex and enhanced RNA synthesis of both the wild and vaccine strain of MeV, as in the case of hsp72 for a vaccine strain. In such a model, too high of a level of intracellular Prdx1 would reduce viral growth because its excessive competition keeps RdRp from interacting with the nucleocapsids sufficiently. Prdx1 is expressed constitutively and abundantly in various cells, including HEK293-SLAM cells. This might be the reason why the reduction of MeV growth indicated by overexpression of Prdx1 was not a large effect (Fig. 7).

A luciferase gene was inserted between the N and P genes in MeV-luc; however, the extent of reduction of *luc* mRNA expression was greater than that of P mRNA and similar to that of L mRNA (Fig. 6). Furthermore, the absolute expression level of *luc* mRNA was also lower than that of P mRNA and similar to that of L mRNA (data not shown). The luc gene in MeV-luc might be recognized inefficiently by RdRp, and its transcription might be easily posed compared with viral genes.

Prdx1 suppression in HEK293-SLAM cells resulted in significant reduction in viral RNA synthesis and release of infectious progeny virus. As Prdx1 is expressed constitutively and abundantly in normal conditions in various cells, our results indicated that Prdx1 was one of the inherent factors for RNA synthesis. Surface plasmon resonance analysis showed that the binding affinity of Prdx1 to N_{TAIL} was approximately 40-fold lower than that of P protein to N_{TAIL} (Fig. 2A), suggesting that Prdx1 might be effective in MeV RNA synthesis at the early stage of infection when the amount of cellular Prdx1 is much greater than that of the viral P protein.

It has remained to be solved which amino acids on N_{TAIL} and Prdx1 were involved in their interaction. The identification of them would lead to direct evidence of the relation between the physical interaction of Prdx1 with the N protein and the enhancement of MeV RNA synthesis.

ACKNOWLEDGMENTS

We thank H. Fukuda and S. Ohmi, Institute of Medical Sciences, University of Tokyo, for MALDI-TOF MS analysis.

This study was supported by a Grant-in-Aid from the Ministry of Education, Science, Culture and Sports, Japan.

REFERENCES

1. **Bose, S., M. Manjula, P. Bates, N. Joshi, and A. K. Banerjee.** 2003. Requirement for cyclophilin A for the replication of vesicular stomatitis virus New Jersey serotype. J. Gen. Virol. **84:**1687–1699.
2. **Bourhis, J. M., et al.** 2004. The C-terminal domain of measles virus nucleoprotein belongs to the class of intrinsically disordered proteins that fold upon binding to their physiological partner. Virus Res. **99:**157–167.
3. **Bourhis, J. M., et al.** 2005. The intrinsically disordered C-terminal domain of the measles virus nucleoprotein interacts with the C-terminal domain of the phosphoprotein via two distinct sites and remains predominantly unfolded. Protein Sci. **14:**1975–1992.
4. **Bourhis, J. M., B. Canard, and S. Longhi.** 2006. Structural disorder within the replicative complex of measles virus: functional implications. Virology **344:**94–110.
5. Reference deleted.
6. **Bryce, J., C. Boschi-Pinto, K. Shibuya, and R. E. Black.** 2005. WHO estimates of the causes of death in children. Lancet **365:**1147–1152.
7. **Carsillo, T., Z. Traylor, C. Choi, S. Niewiesk, and M. Oglesbee.** 2006. Hsp72, a host determinant of measles virus neurovirulence. J. Virol. **80:**11031–11039.
8. **Carsillo, T., X. Zhang, D. Vasconcelos, S. Niewiesk, and M. Oglesbee.** 2006. A single codon in the nucleocapsid protein C terminus contributes to in vitro and in vivo fitness of Edmonston measles virus. J. Virol. **80:**2904–2912.
9. **Chung, C.-S., et al.** 2006. Vaccinia virus proteome: identification of proteins in vaccinia virus intracellular mature virion particles. J. Virol. **80:**2127–2140.
10. **Geiben-Lynn, R., et al.** 2003. HIV-1 antiviral activity of recombinant natural killer cell enhancing factors, NKEF-A and NKEF-B, members of the peroxiredoxin family. J. Biol. Chem. **278:**1569–1574.
11. **Hoshino, I., et al.** 2005. Histone deacetylase inhibitor FK228 activates tumor suppressor Prdx1 with apoptosis induction in esophageal cancer cells. Clin. Cancer Res. **11:**7945–7952.
12. **Iverson, L. E., and J. K. Rose.** 1981. Localized attenuation and discontinuous synthesis during vesicular stomatitis virus transcription. Cell **23:**477–484.
13. **Johansson, K., et al.** 2003. Crystal structure of the measles virus phosphoprotein domain responsible for the induced folding of the C-terminal domain of the nucleoprotein. J. Biol. Chem. **278:**44567–44573.
14. Reference deleted.
15. **Kingston, R. L., W. A. Baase, and L. S. Gay.** 2004. Characterization of nucleocapsid binding by the measles virus and mumps virus phosphoproteins. J. Virol. **78:**8630–8640.
16. **Kingston, R. L., D. J. Hamel, L. S. Gay, F. W. Dahlquist, and B. W. Matthews.** 2004. Structural basis for the attachment of a paramyxoviral polymerase to its template. Proc. Natl. Acad. Sci. U. S. A. **101:**8301–8306.
17. **Kobune, F., et al.** 1996. Nonhuman primate models of measles. Lab. Anim. Sci. **46:**315–320.
18. **Kobune, F., et al.** 2007. A novel monolayer cell line derived from human umbilical cord blood cells shows high sensitivity to measles virus. J. Gen. Virol. **88:**1565–1567.
19. **Livak, K. J., and T. D. Schmittgen.** 2001. Analysis of relative gene expression data using real-time quantitative PCR and the $2^{-\Delta\Delta CT}$ method. Methods **25:**402–408.
20. **Morrison-Bogorad, M., A. L. Zimmerman, and S. Pardue.** 1995. Heat-shock 70 messenger RNA levels in human brain: correlation with agonal fever. J. Neurochem. **64:**235–246.
21. **Mu, Z. M., X. Y. Yin, and E. V. Prochownik.** 2002. Pag, a putative tumor suppressor, interacts with the Myc box II domain of c-Myc and selectively alters its biological function and target gene expression. J. Biol. Chem. **277:**43175–43184.
22. **Netto, L. E. S., H. Z. Chae, S. W. Kang, S. G. Rhee, and E. R. Stadtman.** 1996. Removal of hydrogen peroxide by thiol-specific antioxidant enzyme (TSA) is involved with its antioxidant properties: TSA possesses thiol peroxidase activity. J. Biol. Chem. **271:**15315–15321.
23. **Neumann, C. A., et al.** 2003. Essential role for the peroxiredoxin Prdx1 in erythrocyte antioxidant defence and tumour suppression. Nature **424:**561–565.
24. **Plumet, S., and D. Gerlier.** 2005. Optimized SYBR green real-time PCR assay to quantify the absolute copy number of measles virus RNAs using gene specific primers. J. Virol. Methods **128:**79–87.
25. **Prospéri, M. T., D. Ferbus, I. Karczinski, and G. Goubin.** 1993. A human cDNA corresponding to a gene overexpressed during cell proliferation encodes a product sharing homology with amoebic and bacterial proteins. J. Biol. Chem. **268:**11050–11056.
26. **Rhee, S. G., H. Z. Chae, and K. Kim.** 2005. Peroxiredoxins: a historical overview and speculative preview of novel mechanisms and emerging concepts in cell signaling. Free Radic. Biol. Med. **38:**1543–1552.
27. **Sato, H., et al.** 2008. Measles virus induces cell-type specific changes in gene expression. Virology **375:**321–330.
28. **Seo, M. S., et al.** 2000. Identification of a new type of mammalian peroxiredoxin that forms an intramolecular disulfide as a reaction intermediate. J. Biol. Chem. **275:**20346–20354.
29. **Su, C. Y., et al.** 1999. A physiologically relevant hyperthermia selectively activates constitutive hsp70 in H9c2 cardiac myoblasts and confers oxidative protection. J. Mol. Cell. Cardiol. **31:**845–855.
30. **Vasconcelos, D. Y., E. Norrby, and M. J. Oglesbee.** 1998. The cellular stress response increases measles virus-induced cytopathic effect. J. Gen. Virol. **79:**1769–1773.
31. **Vasconcelos, D., X. H. Cai, and M. Oglesbee.** 1998. Constitutive overexpression of the major inducible 70 kDa heat shock protein mediates large plaque formation by measles virus. J. Gen. Virol. **79:**2239–2247.
32. **Watanabe, A., et al.** 2010. CD147/EMMPRIN acts as a functional entry receptor for measles virus on epithelial cells. J. Virol. **84:**4183–4193.
33. **Wen, S.-T., and R. A. Van Etten.** 1997. The *PAG* gene product, a stress-induced protein with antioxidant properties, is an Abl SH3-binding protein and a physiological inhibitor of c-Abl tyrosine kinase activity. Genes Dev. **11:**2456–2467.
34. **Zhang, X., et al.** 2002. Identification and characterization of a regulatory domain on the carboxyl terminus of the measles virus nucleocapsid protein. J. Virol. **76:**8737–8746.
35. **Zhang, X., et al.** 2005. Hsp72 recognizes a P binding motif in the measles virus N protein C-terminus. Virology **337:**162–174.